Insufficient Hartree–Fock Exchange in Hybrid DFT Functionals Produces Bent Alkynyl Radical Structures

ARTICLE *in* JOURNAL OF PHYSICAL CHEMISTRY LETTERS · JANUARY 2012

Impact Factor: 7.46 · DOI: 10.1021/jz201564g

4 AUTHORS, INCLUDING:

John Andrew Keith
University of Pittsburgh
50 PUBLICATIONS **1,025** CITATIONS

SEE PROFILE

Michele Pavone
University of Naples Federico II
58 PUBLICATIONS **1,185** CITATIONS

SEE PROFILE

THE JOURNAL OF PHYSICAL CHEMISTRY Letters

Letter

pubs.acs.org/JPCL

Insufficient Hartree−Fock Exchange in Hybrid DFT Functionals Produces Bent Alkynyl Radical Structures

Victor B. Oyeyemi,[†] John A. Keith,[‡] Michele Pavone,[‡,⊥] and Emily A. Carter*[,‡,§,∥]

Departments of [†]Chemical and Biological Engineering and [‡]Mechanical and Aerospace Engineering, [§]Program in Applied and Computational Mathematics, and [∥]Andlinger Center for Energy and the Environment, Princeton University, Princeton, New Jersey, 08544-5263, United States

Supporting Information

ABSTRACT: Density functional theory (DFT) is often used to determine the electronic and geometric structures of molecules. While studying alkynyl radicals, we discovered that DFT exchange-correlation (XC) functionals containing less than ∼22% Hartree−Fock (HF) exchange led to qualitatively different structures than those predicted from *ab initio* HF and post-HF calculations or DFT XCs containing 25% or more HF exchange. We attribute this discrepancy to rehybridization at the radical center due to electron delocalization across the triple bonds of the alkynyl groups, which itself is an artifact of self-interaction and delocalization errors. Inclusion of sufficient exact exchange reduces these errors and suppresses this erroneous delocalization; we find that a threshold amount is needed for accurate structure determinations. Below this threshold, significant errors in predicted alkyne thermochemistry emerge as a consequence.

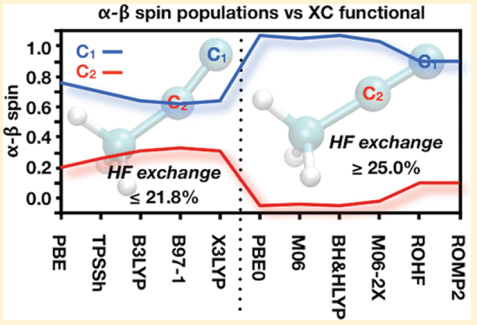

SECTION: Molecular Structure, Quantum Chemistry, General Theory

Computational modeling plays an important role in combustion studies and predicting properties of fuels. This modeling requires accurate thermochemical properties of species such as bond dissociation energies (BDEs), which are often obtained from ab initio quantum chemistry methods.[1] However, before reliable BDEs can be calculated, molecular structures of the relevant species must be obtained with reasonable accuracy.

Alkynyl radicals are participants in soot formation[2,3] and interstellar chemistry,[4] but details of their properties and reactivity have been challenging to elucidate. For example, accurate electronic structures for these radicals are often difficult to characterize, and the associated alkyne photodissociation branching ratios have been the subject of ongoing controversy.[5] Ethynyl ($^2\Sigma^+$)[6] and 1-propynyl ($^2A_1$)[7] ground-state geometries are established from experiment, and their symmetries signify that the R−C−C angles in these two radicals are linear. We are not aware of experimental studies characterizing geometries of larger alkynyl radicals. However, one might expect that, like ethynyl and 1-propynyl, larger radicals also have locally linear R−C≡C• structures.

While investigating BDEs of fuel molecules,[8] we found that some commonly used density functional theory (DFT)[9−11] exchange-correlation (XC) functionals predict qualitatively different structures for these radicals. Ab initio Hartree−Fock (HF)[12−14] and second-order perturbation theory (MP2),[15,16] as well as some hybrid DFT XC functionals, predict linear R−C≡C• moieties (R−C−C bond angle of ∼180°), but other DFT XCs (including PBE, X3LYP, and B3LYP) produce structures with noticeably nonlinear bond angles of ∼160°.

This spurious bending was observed previously in calculations using the B3LYP XC functional.[17−21] Theoretical studies reporting bent 1-propynyl structures note that single-reference methods converge to a low-lying ^2E state, which is then subject to symmetry breaking and Jahn−Teller distortion.[7,18,19] Eisfeld demonstrated the need for detailed multireference configuration interaction calculations to obtain the correct ground state electronic structure of 1-propynyl.[5] However, multireference effects cannot be fully responsible for bent geometries, as some single reference methods also predict linear R−C−C bond angles. We investigated this subject further to alert the chemical community that alkynyl geometries from some commonly used XC functionals are qualitatively inaccurate due to erroneous electron delocalization, and we show that this artifact is a consequence of insufficient inclusion of exact exchange. One serious outcome of predicting bent instead of linear geometries for these radicals are that significant errors arise in predictions of alkyne BDEs, as we demonstrate here.

Geometry optimizations and vibrational frequency calculations on the four alkynyl radicals shown in Figure 1 were run using the GAMESS-US[22,23] computational chemistry program. To allow full geometric relaxation, symmetry was not imposed

Received: November 27, 2011
Accepted: January 6, 2012

   dx.doi.org/10.1021/jz201564g | *J. Phys. Chem. Lett.* 2012, 3, 289−293

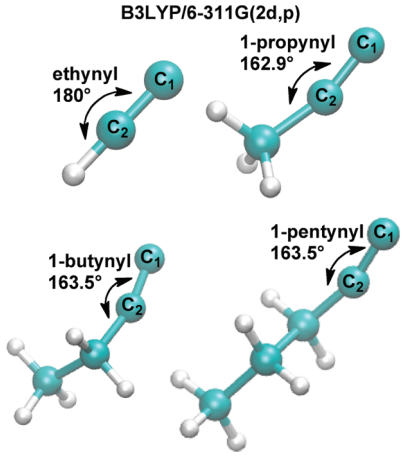

Figure 1. U-DFT-B3LYP/6-311G(2d,p) structures for alkynyl radicals. This model chemistry predicts alkynyl structures with bond angles of 180° for ethynyl and ~163° for the other radicals.

in calculations. We optimized geometries using restricted open-shell HF (ROHF),[13] restricted open-shell MP2 (ROMP2),[15,16] and unrestricted DFT (U-DFT) with a selection of nine different XC functionals, each consisting of different mathematical constructions and amounts of exact exchange. Restricted open-shell DFT and unrestricted HF were not used because the former introduces formally unjustified constraints into the Kohn–Sham determinant,[24] and the latter suffers from much larger spin contamination errors than U-DFT.[25] In all calculations, U-DFT converged to geometries with minimal spin contamination (S^2 = 0.75–0.79). Table 1 shows the XC functionals used in this study along with the percentage of HF exchange (X) they contain. The 6-311G(2d,p)[26] Pople basis set and the Dunning basis sets[27−29] cc-pVDZ, cc-pVTZ, cc-pVQZ, aug-cc-pVDZ, and aug-cc-pVTZ were used for geometry optimizations and frequency calculations. See Supporting Information for details of algorithms and optimization parameters used.

After determining the molecular structures, BDEs were calculated using our complete basis set extrapolated multi-reference singles and doubles configuration interaction scheme (MRSDCI/cc-pV∞Z) previously described.[8] This scheme uses complete active space self-consistent field (CASSCF)[30] wave function references for the MRSDCI calculations. The minimal version of this method was used for the BDEs (D_e and D_{298}) reported below. Here, the CASSCF active space at the equilibrium geometry is composed of the two electrons involved in the breaking bond and their corresponding bonding and antibonding orbitals. The corresponding active space at the dissociation limit (taken here to be 10 Å separation) is composed of two singly occupied orbitals, one on each radical fragment (here, the alkynyl radical and an H atom). Only valence electrons are correlated in the MRSDCI/cc-pV∞Z calculations. The computed frequencies are used to calculate zero point energies (ZPEs) and thermal corrections (TCs) to the BDEs using the ideal gas, rigid rotor approximation.[31]

Single reference *ab initio* ROHF and ROMP2 calculations on alkynyl radicals (R–C≡C•; R = H, CH_3, C_2H_5, C_3H_7) predict ethynyl and 1-propynyl to be linear, while bond angles for 1-butynyl (ROHF = 179.2°; ROMP2 = 176.4°) and 1-pentynyl (ROHF = 179.1°; ROMP2 = 175.1°) were linear to within 1–5°. This is consistent with the expectation that the triply bonded carbon atoms should be *sp*-hybridized. The differences in ROMP2 energy between fully linear and the optimized nearly linear geometry were very small: 0.03 kcal/mol for 1-butynyl and 1-pentynyl, confirming the linear/quasilinear geometry predicted with ROHF theory (and the flat nature of the potential energy surface near 180°). By contrast, Figure 1 shows the four alkynyl radicals optimized at the U-DFT-B3LYP/6-311G(2d,p) level. Note that these would be the same geometries obtained from the popular CBS-QB3 method.[32] All structures have R–C–C bond angles of ~163° except the ethynyl radical, which is predicted to be linear. Results were robust with respect to using bent or linear initial guesses for all four radicals, and tests on the representative case of 1-propynyl verified that tighter energy and geometry convergence criteria and denser DFT grids did not change the predicted structures (see Supporting Information). Geometry optimizations using Dunning-type basis sets larger than cc-pVDZ and up to cc-pVQZ and aug-ccpVTZ all converged to the same geometries for the representative cases of ethynyl and 1-propynyl. Thus, these structures are not likely to be artifacts of basis set choice. The differences in B3LYP/6-311G(2d,p) energy between fully linear and the optimized bent geometries were significantly larger than in the ROMP2 cases: 2.03 kcal/mol for 1-propynyl and 1.93 kcal/mol for 1-butynyl and 1-pentynyl, suggesting that the bent structure in each case is a robust minimum.

We then optimized the structures of the four alkynyl radicals with the U-DFT XC functionals listed in Table 1 using the 6-311G(2d,p) basis set. Several of the selected DFT XC functionals share common features. The hybrid-GGA PBE0 functional is the same as the GGA PBE functional except the former has 25% HF exchange (X = 25%) while the latter has none. Hybrid-GGA BH&HLYP (X = 50%) and hybrid-GGA B3LYP (X = 20%) are likewise very similar to each other except for their value of X, as are hybrid meta-GGAs M06 (X = 27%) and M06-2X (X = 54%). However, hybrid-GGAs X3LYP (X = 21.8%), B97-1 (X = 21%), and hybrid-meta GGA

Table 1. DFT XC Functionals Used in This Study

functional	type	X (%)	exchange functional	correlation functional	ref.
PBE	GGA	0.0	Perdew–Burke–Ernzerhof	Perdew–Burke–Ernzerhof	33
TPSSh	hybrid-meta-GGA	10.0	Tao–Perdew–Staroverov–Scuseria	Tao–Perdew–Staroverov–Scuseria	34
B3LYP	hybrid-GGA	20.0	Becke88	Lee–Yang–Parr	35, 36
B97-1	hybrid-GGA	21.0	B97-1	B97-1	37
X3LYP	hybrid-GGA	21.8	Becke88 + Perdew–Wang91	Lee–Yang–Parr	38
PBE0	hybrid-GGA	25.0	Perdew–Burke–Ernzerhof	Perdew–Burke–Ernzerhof	39
M06	hybrid-meta-GGA	27.0	M06	M06	40
BH&HLYP	hybrid-GGA	50.0	Becke 88	Lee–Yang–Parr	22, 23, 36, 41
M06-2X	hybrid-meta-GGA	54.0	M06-2X	M06-2X	40

dx.doi.org/10.1021/jz201564g | J. Phys. Chem. Lett. 2012, 3, 289–293

TPSSh (X = 10%) have different formulations more distinctive from other functionals. Despite the differences in functionals, calculations on alkynyl radicals yielded two categories of minimum energy structures: those that are linear or near linear (with an R−C−C bond angle of 176.2−180°), and those that are noticeably bent (with an R−C−C bond angle of 160.4°−165.4°).

An explanation emerges upon plotting the R−C≡C• bond angle against X, the percentage of HF exchange (Figure 2).

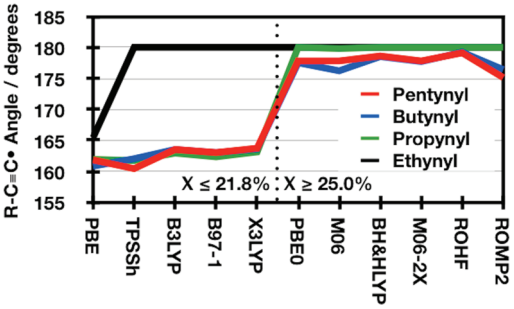

Figure 2. R−C≡C• bond angles for alkynyl radicals. The horizontal axis lists levels of theory in order of increasing percentage of HF exchange (see Table 1). XC functionals with ≥25% HF exchange predict linear ethynyl and 1-propynyl structures and nearly linear 1-butynyl and 1-pentynyl structures.

Here, one clearly sees that all methods that utilize ≥25% HF exchange (DFT with PBE0, M06, BH&HLYP, or M06-2X XC functionals; ROHF; and ROMP2) predict essentially linear alkynyl radical structures regardless of whether the XC functional is a hybrid-GGA or a hybrid-meta-GGA. However, the DFT XCs with less than this amount of HF exchange (PBE, TPSSh, B3LYP, B97-1, and X3LYP) predict bent 1-propynyl, 1-butynyl, and 1-pentynyl radical structures with an R−C−C bond angle of ∼163° regardless of whether the XC functional is a pure GGA, hybrid-GGA, or a hybrid-meta-GGA. For ethynyl, all XC functionals found linear structures except for PBE, for which the structure was bent (165.4°) due again to a very flat potential energy surface: the energy difference between linear and bent structures is only 0.08 kcal/mol (see Supporting Information). The very flat potential energy surface arising from PBE indicates it is not suitable for structural determinations of these radicals.

Insight into the XC trend above may be gleaned by examining the electronic spin density differences ($\alpha-\beta$) from Löwdin[42] populations at the terminal carbon, C_1, and at the other triply bonded carbon, C_2. For a radical localized at C_1, $\alpha-\beta$ will be 1.0 since this site has an excess of 1 electron. For a case involving radical delocalization across the triple bond, $\alpha-\beta$ on C_1 will be less than 1.0, and a significant build-up of spin should be found on C_2. Our results for spin density differences are shown in Figure 3. The observed trend here matches that seen in Figure 2. All methods that predict linear structures have spin density differences of ∼1.0 at C_1 and ∼0.0 at C_2, indicating a localized radical on C_1. For the bent cases, around 30% percent of the spin density migrates from the terminal C_1 to the adjacent C_2 (see Supporting Information for a full table of spin density difference values). Thus, we attribute the bending to delocalization of the lone electron, which causes rehybridization of both C atoms to sp^2, leading to bending at C_2. The delocalization is caused by the well-known problem with pure DFT XC functionals of self-interaction and delocalization

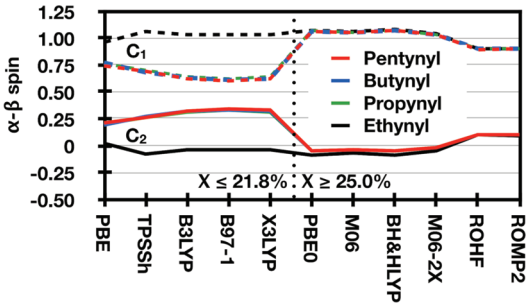

Figure 3. Net spin density at the radical site (C_1, dashed line) and the central carbon (C_2, solid line) of alkynyl (R−C≡C•) radicals. The horizontal axis lists levels of theory in order of increasing percentage of HF exchange (see Table 1). XC functionals with ≥25% HF exchange predict a localized radical on C_1, whereas those with ≤21.8% HF exchange show radical delocalization across C_1 and C_2.

errors.[43] These errors have been implicated in several unphysical DFT predictions (see refs 44, 45, and the references therein), but the full extent of their manifestation in common applications is not established. The self-interaction and delocalization errors produce extraneous electron repulsion (the radical electron interacts with itself) not canceled by exact exchange interactions. To minimize this spurious extra electron repulsion, the radical electron spreads out.

Based on results shown in Figure 3, it is clear that the values of X, the spin orbital populations, and the structures of 1-propynyl, 1-butynyl, and 1-pentynyl are interrelated as explained above. Ethynyl is an exception, however. Figure 3 shows little to no electron delocalization in ethynyl, and all DFT XC functionals (except for PBE) predict linear ethynyl structures. Since we see little evidence of electron delocalization to the alkyl group (see Supporting Information), another factor seems to keep ethynyl linear.

Our best explanation for ethynyl's tendency to stay linear while the others bend for a certain class of XC functionals invokes chemical bonding principles. In these alkynyl radicals, an sp-hybridized C_2 is either bound to an H atom (in ethynyl) or to an sp^3 carbon (in 1-propynyl, 1-butynyl, or 1-pentynyl). In the latter cases, the sp^3 carbon would prefer to bond to C_2 when C_2 is hybridized with substantial p character to maximize its overlap. The spurious radical electron delocalization induces rehybridization (i.e., symmetry-breaking) to incorporate more p character to C_2 ($sp \rightarrow sp^2$), thereby producing bent structures. On the other hand, the H atom, which forms bonds with only an s orbital, would prefer to bond to C_2 when C_2 is hybridized with substantial s character. In this case, the character of the normally sp-hybridized C_2 remains intact and that bonding interaction appears to be enough to counteract the self-interaction/delocalization error driving force in most DFT XC functionals and maintain a linear ethynyl structure.

Ultimately, our goal was to ascertain the significance of these spuriously bent structures on predictions of their thermochemistry. Table 2 shows the energy components needed to calculate (MRSDCI/cc-pV∞Z)[8] alkyne RCC-H BDEs, using geometries from calculations incorporating different quantities of exact exchange (B3LYP, M06-2X, and HF as representatives) for ethyne, propyne, butyne, and their corresponding radicals. Table 2 includes energy contributions due to differences in TCs and ZPEs (reported as the sum of the TCs/ZPEs of the separated radical fragments minus the TC/ZPE of the molecule at equilibrium) as well as their D_e values, the electronic energy

dx.doi.org/10.1021/jz201564g | J. Phys. Chem. Lett. 2012, 3, 289−293

Table 2. Alkyne C−H D_{298}s and Their Energy Components[a] Calculated from Single Point MRSDCI/cc-pV∞Z D_es and from Geometries and Vibrational Frequencies Computed Using the Listed Level of Theory with the 6-311G(2d,p) Basis Set.[b]

		absolute energies (kcal/mol)		
	geometry	ethyne HCC-H	propyne H_3CCC-H	butyne H_3CCH_2CC-H
$\Delta H_{0\rightarrow 298K}$	B3LYP	1.7	**1.5**	**1.5**
	M06−2X	1.5	1.5	1.4
	HF	1.4	1.4	1.4
ΔZPE	B3LYP	−8.0	**-8.5**	**-8.5**
	M06-2X	−7.2	−6.8	−7.0
	HF	−6.9	−6.6	−6.6
D_e	B3LYP	140.1	**143.4**	**143.4**
	M06-2X	140.1	139.8	139.3
	HF	140.2	139.9	139.3
D_{298}	B3LYP	133.9 (133.5)[c]	**136.4**	**136.4**
	M06-2X	134.4	134.5	133.8
	HF	134.7	134.6	134.1
	expt.	133.3[d]		

[a] $\Delta H_{0\rightarrow 298K}$/ΔZPE, the sum of the TCs/ZPEs of the separated radical fragments minus the TC/ZPE of the molecule in its equilibrium geometry, and Born−Oppenheimer BDEs, D_e. [b] Calculations on bent geometries are labeled in bold. Vibrational frequencies used in evaluating $\Delta H_{0\rightarrow 298K}$ and ΔZPE were scaled by 0.99 (ref 32) for B3LYP, 0.94(scale factor optimized for M06-2X/6-31+G(d,p)[46]) for M06-2X, and 0.91(scale factor optimized for R(O)HF/6-311G-(d,p)[47]) for R(O)HF. MRSDCI/cc-pV∞Z D_es and D_{298}s are obtained correlating only the valence electrons. [c] The D_{298} for the C−H bond in ethyne was calculated as 133.5 kcal/mol when a four electron in four orbital active space was used. This active space is made up of the degenerate C−H σ and σ^* bonds and the four C−H bonding electrons. The larger active space reduces the deviation of the computed D_{298} relative to experiment to +0.2 kcal/mol.[8] [d] Reference 48.

change upon bond dissociation. As mentioned earlier, B3LYP predicts a linear structure for ethynyl and bent structures for 1-propynyl and 1-butynyl, while ROHF and M06-2X calculations predict linear structures for all three alkynyl radicals. Bent and linear structures show little difference in their TCs, but their ZPEs differ by more than 1 kcal/mol. D_{298}s are most affected by D_e values, where the bent structures result in values 3.6−4.1 kcal/mol different from those calculated from linear geometries. Because of fortuitous error cancellations between underestimated (negative) ZPE corrections and overestimated (positive) D_e values, the overall D_{298} values between linear and bent structures differ by 1.8−2.6 kcal/mol, which remains a significant error.

In conclusion, we have identified a class of molecules where some popular DFT XC functionals fail to predict accurate geometries. Our analysis shows that this is a result of electron delocalization from the carbon radical center to the adjacent *sp*-hybridized carbon atom, which changes its hybridization to be more like sp^2, thereby producing bent structures. This delocalization occurs only when the percentage of HF exchange in the XC functional is below 25%; however, this threshold includes the ubiquitously used B3LYP XC functional. Thus, only functionals with larger nonlocal exchange components should be used to study alkynyl radicals, since not doing so leads not only to incorrect structures but also to ∼3 kcal/mol errors in thermochemistry, as demonstrated here for alkyne C−H bond energies. We would not be surprised to find similar inaccuracies for other classes of molecules susceptible to spurious electron delocalization.

■ ASSOCIATED CONTENT

Supporting Information

Details of geometry optimization and frequency calculations, Mulliken spin populations, potential energy surfaces for PBE and ROMP2 calculations. This information is available free of charge via the Internet at http://pubs.acs.org/.

■ AUTHOR INFORMATION

Corresponding Author

*E-mail: eac@princeton.edu.

Permanent Address

[⊥]Department of Chemistry, University of Napoli Federico II, Napoli 80120, Italy.

■ ACKNOWLEDGMENTS

This work was supported by the Combustion Energy Frontier Research Center funded by the U.S. Department of Energy, Office of Science, and the Office of Basic Energy Sciences under Award Number DE-SC0001198. We thank the Environmental Molecular Science Laboratory and the National Energy Research Scientific Computer Center for supercomputer time. We thank Dr. Paul Crider for helpful discussions.

■ REFERENCES

(1) Irikura, K. K.; Frurip, D. J. *Computational Thermochemistry: Prediction and Estimation of Molecular Thermodynamics*; American Chemical Society: Washington, DC, 1998; Vol. *677*.

(2) Crider, P. E.; Castiglioni, L.; Kautzman, K. E.; Neumark, D. M. Photodissociation of the Propargyl and Propynyl (C_3D_3) Radicals at 248 and 193 nm. *J. Chem. Phys.* **2009**, *130*, 044310−044317.

(3) Wheeler, S. E.; Robertson, K. A.; Allen, W. D.; Schaefer.; Bomble, Y. J.; Stanton, J. F. Thermochemistry of Key Soot Formation Intermediates: C_3H_3 Isomers. *J. Phys. Chem. A* **2007**, *111*, 3819−3830.

(4) Kaiser, R. I. Experimental Investigation on the Formation of Carbon-Bearing Molecules in the Interstellar Medium via Neutral−Neutral Reactions. *Chem. Rev.* **2002**, *102*, 1309−1358.

(5) Eisfeld, W. Ab Initio Calculation of Electronic Absorption Spectra and Ionization Potentials of C_3H_3 Radicals. *Phys. Chem. Chem. Phys.* **2005**, *7*, 3924−3932.

(6) Szalay, P. G.; Thøgersen, L. S.; Olsen, J.; Kállay, M.; Gauss, J. Equilibrium Geometry of the Ethynyl (CCH) Radical. *J. Phys. Chem. A* **2004**, *108*, 3030−3034.

(7) Zhou, J.; Garand, E.; Eisfeld, W.; Neumark, D. M. Slow Electron Velocity-Map Imaging Spectroscopy of the 1-Propynyl Radical. *J. Chem. Phys.* **2007**, *127*, 034304−034310.

(8) Oyeyemi, V. B.; Pavone, M.; Carter, E. A. Accurate Bond Energies of Hydrocarbons from Complete Basis Set Extrapolated Multi-Reference Singles and Doubles Configuration Interaction. *ChemPhysChem* **2011**, *12*, 3354−3364.

(9) Hohenberg, P.; Kohn, W. Inhomogeneous Electron Gas. *Phys. Rev.* **1964**, *136*, B864−B871.

(10) Kohn, W.; Sham, L. J. Self-Consistent Equations Including Exchange and Correlation Effects. *Phys. Rev.* **1965**, *140*, A1133−A1138.

(11) Sousa, S. F.; Fernandes, P. A.; Ramos, M. J. General Performance of Density Functionals. *J. Phys. Chem. A* **2007**, *111*, 10439−10452.

(12) Roothaan, C. C. J. New Developments in Molecular Orbital Theory. *Rev. Mod. Phys.* **1951**, *23*, 69−89.

(13) Roothaan, C. C. J. Self-Consistent Field Theory for Open Shells of Electronic Systems. *Rev. Mod. Phys.* **1960**, *32*, 179−185.

(14) Pople, J.; Nesbet, R. Self-Consistent Orbitals for Radicals. *J. Chem. Phys.* **1954**, *22*, 571−572.

(15) Lee, T. J.; Jayatilaka, D. An Open-Shell Restricted Hartree−Fock Perturbation Theory Based on Symmetric Spin Orbitals. *Chem. Phys. Lett.* **1993**, *201*, 1−10.
(16) Lee, T.; Rendell, A.; Dyall, K.; Jayatilaka, D. Open-Shell Restricted Hartree−Fock Perturbation Theory: Some Considerations and Comparisons. *J. Chem. Phys.* **1994**, *100*, 7400−7409.
(17) Lee, G. Substituent Effect on Electron Affinity, Gas-Phase Basicity, and Structure of Monosubstituted Propynyl Radicals and Their Anions: A Theoretical Study. *J. Comput. Chem.* **2009**, *30*, 2181−2186.
(18) Sreeruttun, R. K.; Ramasami, P.; Yan, G.; Wannere, C. S.; Schleyer, P. v. R.; Schaefer, H. F. The Alkylethynyl Radicals, •C≡C−C_nH_{2n+1} (n = 1−4), and Their Anions. *Int. J. Mass Spectrom.* **2005**, *241*, 295−304.
(19) Vereecken, L.; Pierloot, K.; Peeters, J. B3LYP-DFT Characterization of the Potential Energy Surface of the CH($X^2\Pi$) + C_2H_2 reaction. *J. Chem. Phys.* **1998**, *108*, 1068−1080.
(20) Krishtal, S. P.; Mebel, A. M.; Kaiser, R. I. A Theoretical Study of the Reaction Mechanism and Product Branching Ratios of C_2H + C_2H_4 and Related Reactions on the C_4H_5 Potential Energy Surface. *J. Phys. Chem. A* **2009**, *113*, 11112−11128.
(21) Kaiser, R. I.; Zhang, F.; Gu, X.; Kislov, V. V.; Mebel, A. M. Reaction Dynamics of the Phenyl Radical (C_6H_5) with 1-Butyne ($HCCC_2H_5$) and 2-Butyne (CH_3CCCH_3). *Chem. Phys. Lett.* **2009**, *481*, 46−53.
(22) Schmidt, M. W.; Baldridge, K. K.; Boatz, J. A.; Elbert, S. T.; Gordon, M. S.; Jensen, J. H.; Koseki, S.; Matsunaga, N.; Nguyen, K. A.; Su, S.; et al. General Atomic and Molecular Electronic Structure System. *J. Comput. Chem.* **1993**, *14*, 1347−1363.
(23) Gordon, M. S.; Schmidt, M. W. Advances in Electronic Structure Theory: GAMESS a Decade Later. In *Theory and Applications of Computational Chemistry, the First Forty Years*; Dykstra, C. E., Frenking, G., Kim, K. S., Scuseria, G. E., Eds.; Elsevier: Amsterdam, 2005; pp 1167−1189.
(24) Pople, J. A.; Gill, P. M. W.; Handy, N. C. Spin-Unrestricted Character of Kohn−Sham Orbitals for Open-Shell Systems. *Int. J. Quantum Chem.* **1995**, *56*, 303−305.
(25) Wong, M. W.; Radom, L. Radical Addition to Alkenes: An Assessment of Theoretical Procedures. *J. Phys. Chem.* **1995**, *99*, 8582−8588.
(26) Krishnan, R.; Binkley, J.; Seeger, R.; Pople, J. Self-Consistent Molecular Orbital Methods. XX. A Basis Set for Correlated Wave Functions. *J. Chem. Phys.* **1980**, *72*, 650−654.
(27) Dunning, T. H. Gaussian Basis Sets for Use in Correlated Molecular Calculations. I. The Atoms Boron through Neon and Hydrogen. *J. Chem. Phys.* **1989**, *90*, 1007−1023.
(28) Kendall, R.; Dunning, T.; Harrison, R. Electron Affinities of the First Row Atoms Revisited. Systematic Basis Sets and Wave Functions. *J. Chem. Phys.* **1992**, *96*, 6796−6806.
(29) Woon, D.; Dunning, T. Gaussian Basis Sets for Use in Correlated Molecular Calculations. V. Core-Valence Basis Sets for Boron Through Neon. *J. Chem. Phys.* **1995**, *103*, 4572−4585.
(30) Roos, B. O. The Complete Active Space Self-Consistent Field Method and its Applications in Electronic Structure Calculations. In *Advances in Chemical Physics: Ab Initio Methods in Quantum Chemistry - Part 2*; Lawley, K. P., Ed.; John Wiley & Sons: New York, 1987; Vol. *69*; pp 399−445.
(31) McQuarrie, D.; Simon, J. *Molecular Thermodynamics*; University Science Books: Sausalito, CA, 1999.
(32) Montgomery, J. A.; Frisch, M. J.; Ochterski, J. W.; Petersson, G. A. A Complete Basis Set Model Chemistry. VI. Use of Density Functional Geometries and Frequencies. *J. Chem. Phys.* **1999**, *110*, 2822−2827.
(33) Perdew, J. P.; Burke, K.; Ernzerhof, M. Generalized Gradient Approximation Made Simple. *Phys. Rev. Lett.* **1996**, *77*, 3865−3868.
(34) Tao, J.; Perdew, J. P.; Staroverov, V. N.; Scuseria, G. E. Climbing the Density Functional Ladder: Nonempirical Meta−Generalized Gradient Approximation Designed for Molecules and Solids. *Phys. Rev. Lett.* **2003**, *91*, 146401−146404.
(35) Becke, A. D. Density-Functional Thermochemistry 0.3. The Role of Exact Exchange. *J. Chem. Phys.* **1993**, *98*, 5648−5652.
(36) Lee, C.; Yang, W.; Parr, R. G. Development of the Colle−Salvetti Correlation-Energy Formula into a Functional of the Electron Density. *Phys. Rev. B* **1988**, *37*, 785−789.
(37) Hamprecht, F. A.; Cohen, A. J.; Tozer, D. J.; Handy, N. C. Development and Assessment of New Exchange-Correlation Functionals. *J. Chem. Phys.* **1998**, *109*, 6264−6271.
(38) Xu, X.; Goddard, W. A. The X3LYP Extended Density Functional for Accurate Descriptions of Nonbond Interactions, Spin States, and Thermochemical Properties. *Proc. Natl. Acad. Sci. U.S.A.* **2004**, *101*, 2673−2677.
(39) Adamo, C.; Barone, V. Toward Reliable Density Functional Methods without Adjustable Parameters: The PBE0Model. *J. Chem. Phys.* **1999**, *110*, 6158−6170.
(40) Zhao, Y.; Truhlar, D. The M06 Suite of Density Functionals for Main Group Thermochemistry, Thermochemical Kinetics, Noncovalent Interactions, Excited States, and Transition Elements: Two New Functionals and Systematic Testing of Four M06-Class Functionals and 12 Other Functionals. *Theor. Chem. Acc.* **2008**, *120*, 215−241.
(41) Becke, A. D. A New Mixing of Hartree−Fock and Local Density-Functional Theories. *J. Chem. Phys.* **1993**, *98*, 1372−1377.
(42) Löwdin, P. On the Non-orthogonality Problem Connected with the Use of Atomic Wave Functions in the Theory of Molecules and Crystals. *J. Chem. Phys.* **1950**, *18*, 365−375.
(43) Perdew, J. P.; Zunger, A. Self-Interaction Correction to Density-Functional Approximations for Many-Electron Systems. *Phys. Rev. B* **1981**, *23*, 5048−5079.
(44) Gräfenstein, J.; Kraka, E.; Cremer, D. The Impact of the Self-Interaction Error on the Density Functional Theory Description of Dissociating Radical Cations: Ionic and Covalent Dissociation Limits. *J. Chem. Phys.* **2004**, *120*, 524−539.
(45) Haunschild, R.; Henderson, T. M.; Jimenez-Hoyos, C. A.; Scuseria, G. E. Many-Electron Self-Interaction and Spin Polarization Errors in Local Hybrid Density Functionals. *J. Chem. Phys.* **2010**, *133*, 134116.
(46) Zheng, J.; Lynch, B. J.; Zhao, Y.; Truhlar, D. G.*Database of Frequency Scaling Factors for Electronic Structure Methods*; http://comp.chem.umn.edu/database/freq_scale.htm, 2009
(47) *Computational Chemistry Comparison and Benchmark DataBase*, 2006 ed.; NIST: Gaithersburg, MD, 2006 (http://cccbdb.nist.gov/).
(48) Blanksby, S. J.; Ellison, B. G. Bond Dissociation Energies of Organic Molecules. *Acc. Chem. Res.* **2003**, *36*, 255−263.